Tracing the Potential Existence of the Asian Tropopause Aerosol Layer (ATAL) Prior to the Late 1990s through Observations

Corinna Kloss[1,2], Adriana Bossolasco[1,*], Larry Thomason[3], Bernard Legras[4], Gwenaël Berthet[1], Fabrice Jégou[1], Suvarna Fadnavis[5], Pasquale Sellitto[6,7]

[1]Laboratoire de Physique et Chimie de l'Environnement et de l'Espace, CNRS/Université d'Orléans, UMR 7328, Orléans, France
[2]Institute for Energy and Climate – Stratosphere (IEK-7), Forschungszentrum Jülich GmbH, Jülich, Germany
[3]NASA Langley Research Center, Hampton, VA, USA
[4]Laboratoire de Météorologie Dynamique, UMR CNRS 8539, ENS-PSL/ Sorbonne Université/ École Polytechnique, Paris, France
[5]Indian Institute of tropical Meteorology, Pune, India
[6]Laboratoire Interuniversitaire des Systèmes Atmosphériques, UMR CNRS 7583, Université Paris-Est Créteil, Université de Paris, Institut Pierre Simon Laplace (IPSL), Créteil, France
[7]Istituto Nazionale di Geofisica e Vulcanologia, Osservatorio Etneo, Catania, Italy
*now at: Physics Institute of Northwest Argentina (INFINOA) -CONICET (National Council for Scientific and Technical Research) - National University of Tucumán.: Tucumán, Argentina

Key Points:

- Early space-borne observations (SAGE instruments) cannot be used for ATAL evolution studies, contrary to previous claims.
- SAGE lacks sufficient data in the tropics and an effective cloud capture method to reliably detect or exclude the presence of ATAL.
- First model simulations indicate an ATAL signal, without volcanic influence, in 1979 and 1980.

Corresponding author: Corinna Kloss, c.kloss@fz-juelich.de

Abstract

An enhanced aerosol layer, known as the Asian Tropopause Aerosol Layer (ATAL), has been observed within the seasonal Asian monsoon anticyclone (AMA) since the late 1990s. Given the apparently abrupt appearance of this layer based on observations, it has been speculated that it originates from increasing human made emissions in Asia. However, the ATAL confinement is a result of a dynamical feature and does not purely consist of human made components. We herein investigate the possible existence of an ATAL earlier than the late 1990s. We exploit earliest possible, high quality space-based aerosol observations from Stratospheric Aerosol and Gas Experiment, or SAGE (1979-1981), SAGE III/ISS (2017, ongoing) and revisit SAGE II (1984-2005) data analysis. We find that seasonal averaged solar occultation aerosol measurements (past and present) can neither be used to exclude the existence of the ATAL, nor to infer a significant trend. However, first CAM5-MAM7 simulations indicate the presence of an ATAL signal for the tested years 1979 and 1980, with a human made component. We hypothesize that the human made component of the ATAL likely occurred since at least the 1970s, while the natural ATAL component (e.g. from dust) has always existed. Extended simulation based ATAL evolution studies are therefore the most reliable source for early ATAL investigations.

Plain Language Summary

An enhanced aerosol layer in the Upper Troposphere and Lower Stratosphere (UTLS), known as ATAL (Asian Tropopause Aerosol Layer), was discovered during the seasonal Asian monsoon. Initial observations from space-borne aerosol data suggested its first appearance in the late 1990s. However, our study reveals that the data set used (from SAGE instruments) is inadequate for ATAL evolution studies and to conclusively determine its existence. The limited sampling within the Asian monsoon region and cloud filtering procedure do not provide sufficient data points for definitive conclusions. Nevertheless, the dynamical structure leading to an ATAL has always been present, leading us to hypothesize that the non-human-made ATAL component has existed previously. Additionally, our first model simulations for 1979 and 1980 indicate the presence of an ATAL.

1 Introduction

During Northern hemispheric summer the Asian monsoon is associated with the rainy season (June to September). The large scale monsoon convection lifts continental, polluted air masses from the boundary layer to the upper-troposphere/lower-stratosphere (UTLS), where they are trapped within the dynamical boundaries of the Asian monsoon anticyclone (AMA). Deep convection sources for the air within the AMA takes mainly place at the foot hills of the Himalayas and the Sichuan Basin (e.g. Pan et al., 2016; Yuan et al., 2019; Fadnavis et al., 2013). This results in an enhancement of tropospheric trace gases (e.g. Santee et al., 2017) and aerosols (e.g. J.-P. Vernier, Thomason, & Kar, 2011; Yu et al., 2015; Bossolasco et al., 2021) within the AMA. The enhanced aerosol layer observed in the AMA is called the Asian Tropopause Aerosol Layer (ATAL). The ATAL was first reported by J.-P. Vernier, Thomason, and Kar (2011) with satellite-based data (i.e., CALIOP: Cloud-Aerosol Lidar with Orthogonal Polarization). Since then, the existence of the ATAL was detected with multiple other satellite instruments (Stratospheric Aerosol and Gas Experiment, SAGE II: J.-P. Vernier et al. (2015) and Thomason and Vernier (2013), SAGE III/ISS and Ozone Mapping and Profiler Suite, OMPS: Kloss et al. (2019); CRyogenic Infrared Spectrometers and Telescopes for the Atmosphere, CRISTA: Höpfner et al. (2019) and in situ measurements (J.-P. Vernier et al., 2018; Brunamonti et al., 2018; Höpfner et al., 2019; Mahnke et al., 2021; Appel et al., 2022; H. Vernier et al., 2022). Multiple model studies have investigated the composition, source regions and evolution of the ATAL (e.g. Fadnavis et al. (2019)). Based on simulations, which do not

account for the locality of convection, main boundary layer source regions have been found at the Tibetan Plateau, southwest China, southeast Asia and the western Pacific (e.g. Vogel et al., 2015; Fairlie et al., 2020). However, source regions may vary even within each monsoon season, strongly influencing the strength of the ATAL (Vogel et al., 2015). The variability of the strength of the monsoon dynamics is also closely related to the day-to day distribution variability of enhanced trace gases and aerosol in the AMA (e.g. Lau et al., 2018; Hanumanthu et al., 2020; Fadnavis et al., 2017).
The only attempt to investigate the first buildup and year-to-year evolution of the ATAL was made by J.-P. Vernier et al. (2015) (V15), using satellite observations by SAGE II and CALIOP ranging back to 1996. It was concluded, and has been widely accepted afterwards by the scientific community, that the ATAL first appeared in 1998, likely resulting from increasing anthropogenic SO_2 emissions in Asia. However, some doubts remain on why the ATAL would first appear by 1998. Multiple results and arguments point to a possible existence of the ATAL prior to the 1990s:

1. Model studies suggest that the ATAL aerosol is diverse in composition and not completely human-derived: Simulations show multiple types of aerosols within the ATAL including mineral dust, organic aerosol, nitrate, sulfate, and ammonium aerosol, without an exclusive human-derived component (Ma et al., 2019; Yuan et al., 2019; Fairlie et al., 2020; Bossolasco et al., 2021). A model study by Neely et al. (2014) shows that the ATAL might also exist without any emission contributions from Asia. Though, they also show that, for their model setup, without global anthropogenic emissions there would not be an ATAL layer. The model set up in Neely et al. (2014) does not consider ammonium chemistry.
2. Höpfner et al. (2019) detected ammonium nitrate aerosols within the AMA in 1997, using archived satellite data (their Figure 1 with CRISTA-data). For the year 1997, space-borne data analysis in V15 did not identify a significant ATAL signal. In situ mass spectrometry analysis also reveal that the aerosols within the ATAL mainly consisted of ammonium nitrate and organics, during a measurement campaign in 2017 (Appel et al., 2022).
3. Increased anthropogenic emissions in Asia already started in the early 1960s (not the late 1990s) associated with the so-called 'green revolution'. The green revolution describes the introduction of high-yielding crop varieties and massive usage of fertilizers (nitrates), greatly increasing the food production as detailed in Liu et al. (2021) and Pingali (2012). (Smith et al., 2011) show that global SO_2 emissions began increasing around 1850 and peaked in the 1970s and slowly decreased towards the late 1990s. SO_2 emissions in China started exponentially increasing in $\sim$1950. Hence, even if the existence of the ATAL depended on human-made emissions, we would expect an ATAL signal long before the late 1990s.

Within this study we are exploring the existence of the ATAL for years prior to the late 1990, based on earliest possible high quality space borne observations and first respective model simulations. Is it possible that limitations to the data or incomplete analysis hide earlier instances of ATAL?

2 Methods

2.1 SAGE I

The Stratospheric Aerosol and Gas Experiment (SAGE, hereafter referred to as SAGE I) was a solar occultation instrument aboard the Applications Explorer Mission-B (AEM-B) satellite (Chu & McCornick, 1979; McCormick et al., 1979). It delivered measurement profiles from the cloud top (or 0.5 km) up to 40 km altitude of aerosol extinction and concentrations of ozone and nitrogen dioxide from February 1979 to November 1981. Here, we make use of the aerosol extinction data set version 1, given on two wavelengths: 1000

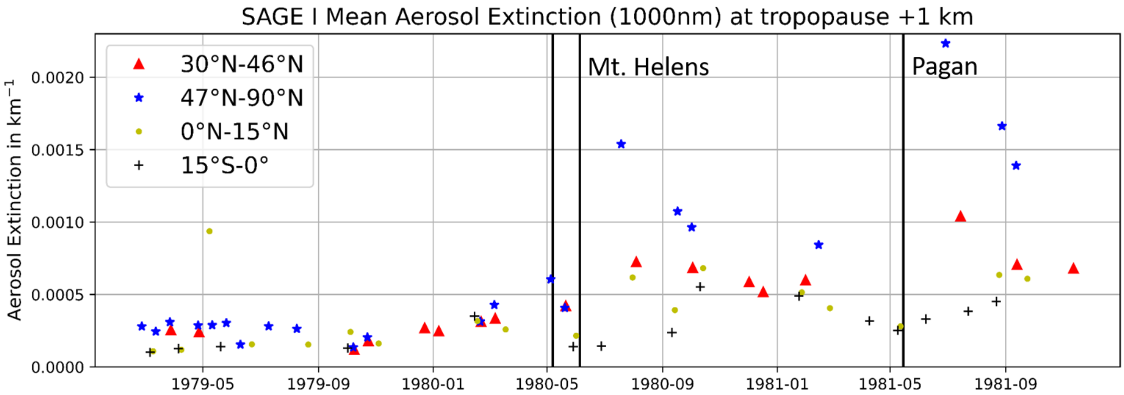

Figure 1. SAGE I (1000 nm) full time series of mean aerosol extinction values between the tropopause and 1 km above the tropopause at different latitude bands. The latitude bands are inspired by the Mt. St. Helens location at 46°N. Significant eruptions by Mt. St. Helens (May 7^{th} and June 5^{th} 1980) and Pagan (May 15^{th} 1981) are indicated with black vertical lines.

nm and 450 nm. However, because the 450 nm channel is only scientifically recommended for cloud filtering (i.e. to use information provided by the ratio of both channels), we do not show averaged profiles from the 450 nm channel (Thomason et al., 1997). SAGE I is reported every half kilometer, with a vertical resolution of around 1 km, similar to SAGE II (Damadeo et al., 2014). In the early 1980s, SAGE I data were validated through a correlative measurement program (P. B. Russell et al., 1984; Kent & McCormick, 1984). Together with SAM II it provides the first space-borne aerosol data set, ranging back as early as 1979. While the SAM II instrument only covered latitudes > 60 degree, SAGE I is the first instrument providing aerosol observations of the Asian monsoon region. SAGE I data released its most recent revision in 1986 and thus the current data set lacks the improved understanding reflected in later data sets like SAGE II v7.0 (Damadeo et al., 2013). Figure 1 shows that timing, location, altitude and magnitude of the aerosol extinction values after the Mt. St. Helens eruption (June 1980) and Alaid, Pagan (April and May 1981) are reasonable, i.e. the data catch larger values associated with the events, and are therefore trustworthy enough for further analysis. Hence, it is the earliest data set that can be used for the investigation of the ATAL.

2.2 SAGE II

The Stratospheric Aerosol and Gas Experiment II (SAGE II) (`https://doi.org/10.5067/ERBS/SAGEII/SOLAR_BINARY_L2-V7.0`) was the follow up instrument to SAGE I, mounted on board the Earth Radiation Budget Satellite (ERBS). It produced ozone, water vapor, nitrogen dioxide and aerosol extinction observations at four wavelengths from 1984 to 2005. Here, we use the aerosol extinction data set version 7.0 at 452 nm, 525 nm and 1020 nm wavelength. With its solar occultation measurement technique, it measured up to 30 profiles per day (15 during sunrise, 15 during sunset), however, during the year 2000 the number of profiles obtained per day decreased to 16. It has a vertical resolution of about 0.5 to 1 km and a variable horizontal resolution, which depends on the angle between the Sun and the direction of motion of the spacecraft (between hundreds and thousands of km^2) (Damadeo et al., 2014). The data set of SAGE II is still extensively used for aerosol extinction observations in the Upper Troposphere and Lower Stratosphere (for example in Thomason et al. (2021); J.-P. Vernier, Thomason, Pommereau, et al. (2011); Thomason and Vernier (2013)) and has also been used for an ATAL evolution investigation of V15, using a specifically designed cloud filter (Thomason & Vernier, 2013). Most (75%) of the SAGE II data record was influenced by atmospheric enhanced aerosol mixing ratios from two 'large' volcanic eruptions (El Chichón in 1982 and Mt. Pinatubo 1991) (Thomason et al., 2021) and is therefore excluded from ATAL investigations. Conservative data quality checks and cloud filtering procedures were conducted according to NASA SAGE-team standards. Other space-borne atmospheric aerosol observations during a siliar time frame as SAGE II exist. Starting from September 1991 until June 2005 the NASA mission Upper Atmosphere Research Satellite (UARS) performed measurements of the Earth's atmosphere, with a special focus on stratospheric ozone. The onboard instrument Halogen Occultation Experiment (HALOE) provided measurements of aerosol extinction, as well as some trace gas information. During the first 4-5 years of measurements the upper atmosphere was loaded with volcanic aerosol and it has been found that UTLS aerosol extinction observations by HALOE are not as reliable as SAGE II observations (Thomason, 2012). UARS, HALOE observations are therefore not included in this study.

2.3 SAGE III/ISS

The Stratospheric Aerosol and Gas Experiment on the International Space Station (SAGE III/ISS) is a solar and lunar occultation instrument, providing profile observations since June 2017. The sampling, measurement technique and resolution is similar to its forerunner SAGE II. For aerosol extinction data, it delivers profile measurements of nine wavelengths. Here, we make use of the 521 nm channel version 5.1 for best comparisons with SAGE II observations. The profile observations are available on a 0.5 km vertical grid.

2.4 CAM5-MAM7

For model simulations of the ATAL in 1979 and 1980 in our study the global Community Earth System Model (CESM1.2) was used, based on the Community Atmospheric Model (CAMS 5.1) with its full chemical core for both troposphere and stratosphere, coupled with the Modal Aerosol Model (MAM7), according to Liu et al. (2012). The setup of the simulations is described in Bossolasco et al. (2021) for a thorough ATAL trend-analysis. The model derives the content of sulfate aerosols, secondary and primary organic aerosols, ammonium particles, and dusts. Nitrate aerosols are not simulated in the model. Because MERRA-2 meteorological input data are not available for 1979, the model is initialized with MERRA instead. However, using MERRA data is not that uncommon for ATAL studies (see, (e.g. Fairlie et al., 2020)). Cloud signatures have been filtered out by selecting simulated profiles only below a given extinction threshold (Bossolasco et al., 2021).

3 Results

3.1 Space-borne ATAL analysis for 1979 (SAGE I)

We use earliest possible space borne observations of stratospheric aerosol within the AMA for ATAL investigations in 1979. With increased aerosol extinction values after the Mt. St. Helens (18/05/1980 at 46°N, 122°W), Ulawun (7/10/1980 at 5°S, 151°E), Alaid (27-30/4/1981 at 51°N, 156°E) and Pagan (15/05/1981 at 18°N, 145°E) eruptions (e.g. J. Russell, 1981), SAGE-I data for 1980 and 1981 are excluded from further analysis (see Figure 1). The year 1979, however, is not impacted by stratospheric aerosol events and can therefore be used as the earliest suitable year. We apply a commonly used technique by averaging over a defined space- and time frame (we choose: 15-45°N, 15-105°E, July and August, a compromise from the choices of Ploeger et al. (2015); Santee et al. (2017) and J.-P. Vernier, Thomason, and Kar (2011)), best representative for the overall location and time of the AMA, using the same cloud- and data quality filtering as

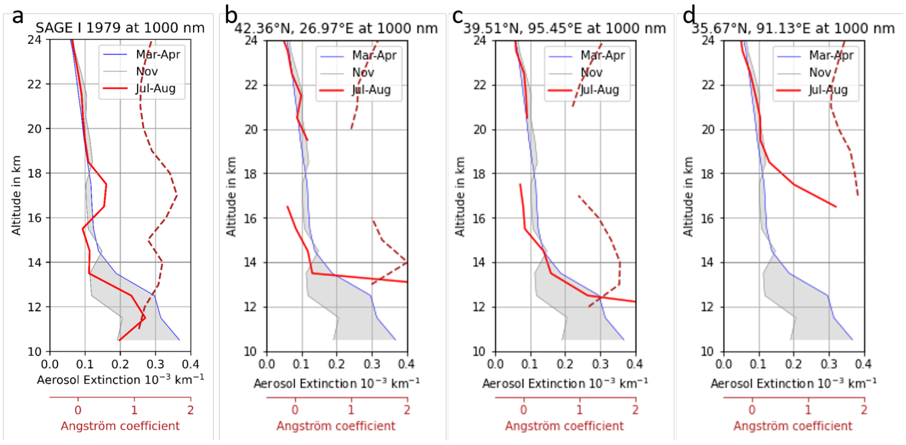

Figure 2. (a) Averaged profile for SAGE I measurements within 15-45°N, 15-105°E in July and August 1979 in red, March and April in blue and November in grey. The grey area represents 'background' conditions (i.e. the area between the blue and grey lines). The Ångström exponent corresponding to the red profile is indicated with the dashed, dark red line. Single profiles averaged for (a) with values at 16.5 km altitude are shown in (b), (c) and (d) in red, with their respective location and Ångström exponent.

applied in V15. The respective averaged profile is presented in Figure 2a, compared to background conditions. The profile shows a clear aerosol extinction enhancement within the AMA at around 17 km altitude. Even the Angstrom exponent, a parameter, which gives indications about the optical thickness and size of observed particles, points to a distinct layer of smaller sized aerosols in the AMA, with values at around 1.9, similar to what was found for SAGE III/ISS ATAL observations for 2017 (Kloss et al., 2019). Hence, first impressions suggest that SAGE I observations show the presence of ATAL in 1979, however, closer investigations of the individual profiles (Figure 2 b, c and d), indicate that the slight aerosol extinction enhancement in Figure 2a only originates from a single profile (Figure 2d). Aerosol extinction measurements below 16 km altitude in Figure 2d are excluded as a result of the applied cloud filter (i.e. the ratio between the extinction channels at 450 to 1000 nm is below 2). Because of the low number and altitude coverage of averaged profiles, we can neither confirm nor exclude the existence of the ATAL with SAGE I observations. However, this result gives motivation to revisit the SAGE II data record, to test the significance of increased aerosol extinction observations, attributed to the ATAL, as observed in V15.

3.2 Space-borne ATAL analysis for 1989 to 2004 and 2017 (SAGE II and SAGE III/ISS)

We use aerosol optical depth (AOD) information from the Global Space-based Stratospheric Aerosol Climatology (GloSSAC) from Kovilakam et al. (2020) (their Figure 15), as well as the complete SAGE II mean aerosol extinction time series at different latitude ranges to identify phases of volcanic influence to be excluded for our ATAL analysis. Hence, nine years of SAGE II satellite observations remain for ATAL investigations (1989, 1990, 1996, 1997, 1998, 1999, 2001, 2003 and 2004), presented in Figure 3 a-i. Compared to V15 and Thomason and Vernier (2013), we use the current (updated) SAGE II data version 7.0 (compared to version 6.2). We, furthermore add the analysis of the most recent suitable year for ATAL investigations with SAGE III/ISS. For the time period 2018 to 2022, stratospheric aerosol in the Asian monsoon region was permanently enhanced due

to several volcanic eruptions (Ambae 2018, Raikoke and Ulawun 2019, Soufriere 2021 and Hunga Tonga 2022). Therefore, only the Asian monsoon season in 2017 is suitable for ATAL investigations. Because the SAGE III/ISS mission only started in June 2017 and Kloss et al. (2019) found significant aerosol enhancements in the AMA region from the Canadian wildfires, starting from mid-August 2017, no background profiles are available for our SAGE III/ISS analysis (Figure 3j).
For most of the investigated years no significant layer of enhanced aerosol extinction values, compared to background conditions is visible. For many of the presented years, however, the Angström exponent points to a layer of smaller sized aerosols (higher Angström exponent values) at AMA altitudes, for most years (clearly visible in Figure 3 a,b,c,d,i and j). The year-to-year SAGE II and SAGE III/ISS ATAL analysis, as presented in Figure 3 gives neither clear indications of a significant ATAL signature nor would it be possible to derive any kind of quantitative estimation or trend of those averaged observations. This uncompelling result, however, gives motivation to study each of the presented ATAL seasons separately, to investigate whether a clear ATAL signature can be found in individual measurement profiles.

Here, we choose to present further investigations for the years 1999 and 2003, for which an ATAL signature of enhanced aerosol extinction values at the tropopause altitude (± 2 km) could be interpreted compared to background conditions from Figure 3. We examine the SAGE II ATAL record for the years 1999 and 2003 by showing the 525 to 1020 nm aerosol extinction ratio versus 1020 nm aerosol extinction coefficient for the respective ATAL altitudes for selected representative periods and spatial extents with no additional filtering (e.g. clouds) in Figure 4. The vertical and horizontal lines (90^{th} percentile of extinction coefficient and median of the 525 to 1020 nm extinction coefficient ratio, respectively) divide the analysis space into 3 regions, an unenhanced region on the left, and two regions on the right both with enhanced aerosol extinction coefficient but divided between higher extinction coefficient ratio and lower extinction coefficient ratio. Data points within the lower right box (Figure 4) are generally consistent with, and consistently interpreted as, aerosol/cloud mixtures (Thomason & Vernier, 2013). Figure 4a shows the resulting distribution for January 1999, a typical month in the ATAL region but away from the expected ATAL season. We see a cluster of data points around an extinction coefficient of 10^{-4} km^{-1}and a ratio of 3. In addition, we see a tail of points stretching from the primary aerosol cluster toward ratios of 1 with extinctions exceeding 0.01 km^{-1}. This tail is observed in the troposphere at all latitudes and is interpreted as aerosol/cloud mixture. The respective analysis for the peak ATAL month, August (7 months later) is shown in Figure 4b. Overall, the figure is extremely similar to the earlier January case except higher number of data points located in the tail suggesting a higher frequency occurrence of clouds in August 1999 in the ATAL region than in January 1999. Overall, 1999 is typical of most years in the SAGE II record away from those strongly affected by the 1991 Mt. Pinatubo eruption. Realistically, we cannot exclude the possibility that some of these 'cloud-aerosol mixture' observations are in reality low ratio/high extinction ATAL enhancements. The fact that all of these enhanced aerosol extinction data points are completely consistent with observations outside of the expected Asian monsoon time frame, highlights the difficulty of identifying ATAL observations in SAGE-like observations. Unlike the behavior shown in 1999, data for July 2003 (Figure 4c) show some aerosol in the high extinction coefficient/high extinction coefficient ratio area, beyond the typical primary aerosol cluster and the aerosol-cloud mixture tail. This suggests the presence of recently nucleated small particles within the ATAL region. However, in this case (2003), these somewhat 'unique data points' are observed far outside the ATAL region: Figure 4d shows the same analysis as Figure 4c except for a box defined by 40-140°W and 20-40°N, (i.e. on the other side of the world). This aerosol is also observed in both regions as early as March 2003 and thus it is almost certainly not associated with ATAL processes.
In general, when we observe rare enhancements of aerosol residing the high extinction/high ratio area of the analyses in the ATAL region and timeframe, they can also be observed

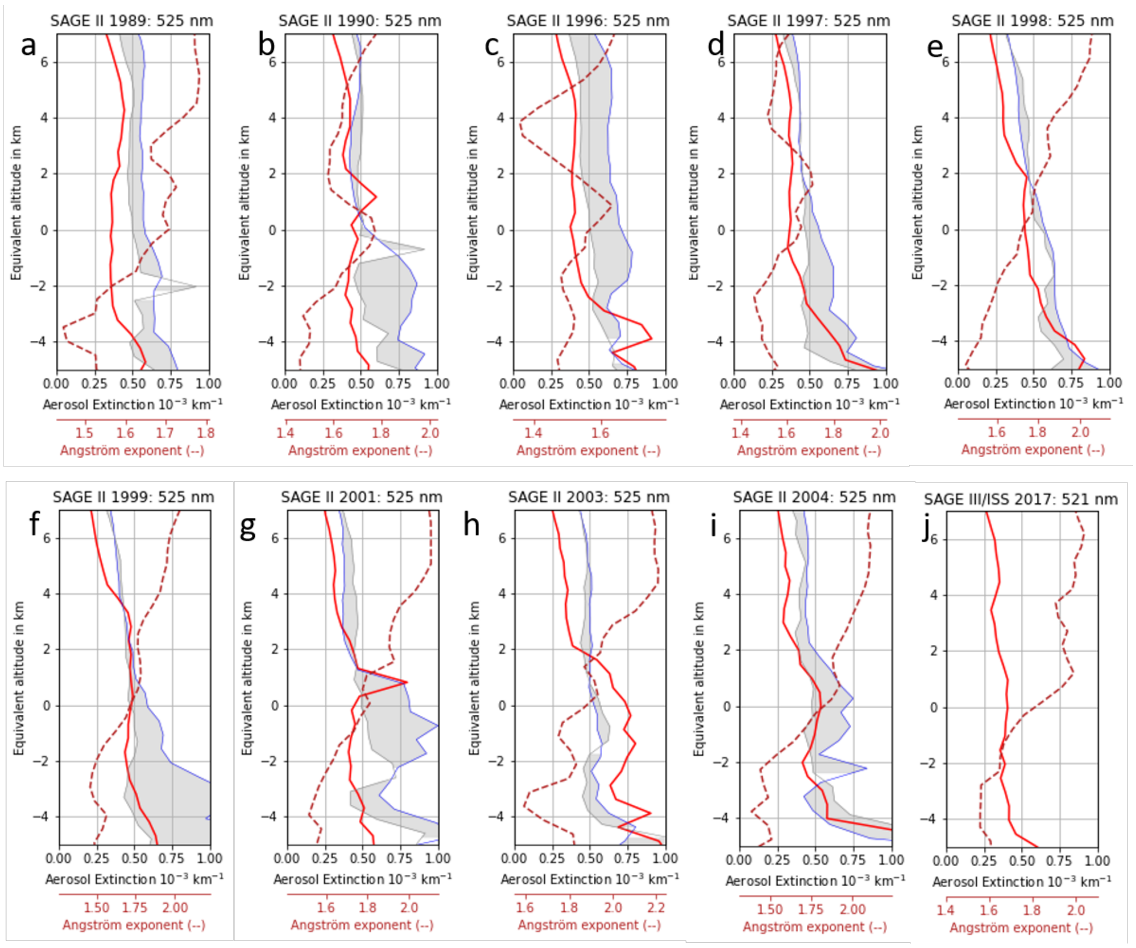

Figure 3. (a)-(i) SAGE II and (j) SAGE III/ISS aerosol extinction (at 525 nm and 521 nm, respectively) profiles averaged over 15-45 °N, 15-105 °E for March/April (blue), November/December (grey) and July/August (Asian monsoon peak time, red) of each year. Equivalent altitude in km are indicated corresponding to the respective tropopause altitudes of the averaged profiles. The grey area represents the span between the blue and gray profiles. (j) The respective profile for 2017 with SAGE III/ISS. For the red curves 36 (a), 28 (b), 56 (c), 55 (d), 53 (e), 44 (f), 35 (g), 19 (h), 14 (i) and 55 (j) profiles with measurement points at 17 km altitude (ATAL altitudes) were averaged. The Ångström exponent of the red curve is indicated with the dark red, dashed line. (j) No background observations are available in 2017 and the time frame is limited to August 15^{th}, because of the arriving aerosol plume from the Canadian fires mid-August in the Asian monsoon region, in the UTLS.

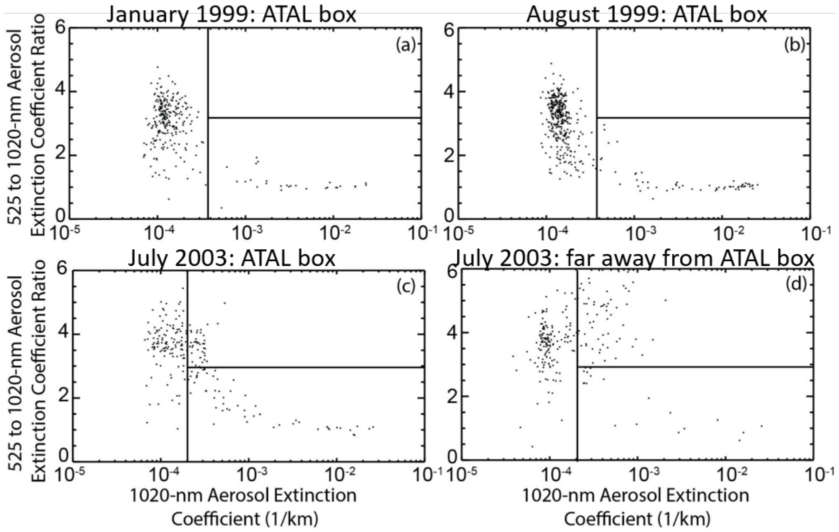

Figure 4. SAGE II 525 to 1020 nm aerosol extinction ratio versus 1020 nm aerosol extinction coefficient between the tropopause minus 3 km and 18 km for (a) January 1999 40-140°E, 20-40°N, (b) July 1999, 40-140°E, 20-40°N, (c) July 2003, 40-140°E, 20-40°N and (d) July 2003, 40-140°W, 20-40°N. No additional cloud filter is applied. Vertical lines represent the 90^{th} percentile of extinction coefficient and vertical lines are located at the median 525 to 1020-nm extinction coefficient ratio.

outside of this window and thus, it is impossible to confidently associate these observations with ATAL processes. At the end, we do not feel that it is possible to identify any specific SAGE II observations as being associated with ATAL related processes with any confidence.
The most recent Asian monsoon time frame, which is not influenced by either extreme fire events or stratospheric volcanic eruptions was in 2017. In July of 2017 aircraft and balloon-based field campaigns (under the EU-project StratoClim and BATAL) took place within the AMA with observations identifying a clear ATAL (Mahnke et al., 2021; J.-P. Vernier et al., 2018). Figure 3j shows no significant aerosol extinction enhancement during the ATAL season in 2017. However, when only averaging mid-August profiles, selected according to the occurring transport barrier at that time (PV criteria, according to Ploeger et al. (2015)), a clear ATAL signal appears, as presented in Figure 2 within Kloss et al. (2019). Hence, even though there is no doubt about the existence of the ATAL during the Asian monsoon season in 2017, the averaged profile of SAGE III/ISS observations with commonly used criteria does not find a clear ATAL structure.

3.3 Simulation-based ATAL analysis for 1979 and 1980 (CAM5-MAM7)

We perform model simulations with the CAM5-MAM7 model as done by Bossolasco et al. (2021). Bossolasco et al. (2021) present a detailed trend analysis of the ATAL, including its spatial distribution and composition. Here, we investigate the ATAL for the complementary years 1979 and 1980. Vertical profiles of the CAM5-MAM7 simulation of aerosol-types-specific concentrations in the ATAL region are shown in Figure 5. A clear ATAL structure is apparent with enhanced mass concentration values at around 16 km altitude in August 1979, with mineral dust (with values up to 250 ng/m^3 at 120 hPa as shown in Figure 6), SOA (secondary organic aerosol) and sulfate (> 100 ng/kg) as dominant ATAL particles. Note that nitrate aerosols are not accounted for in this model. Simulations with and without volcanic emissions (solid vs. dashed lines) exhibit very sim-

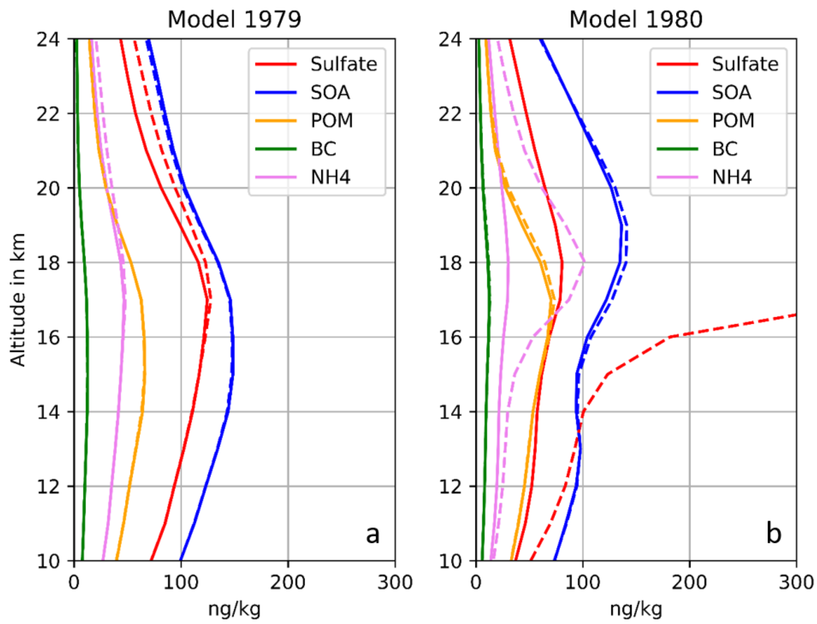

Figure 5. (a) Averaged mass concentration from CAM5-MAM7 model simulations, for August 1979 20-35°N, 60-100°E, with aerosol-type-specific information: sulfate particles (red), SOA (blue), POM (yellow), BC (green) and Ammonium (magenta). Dust is not shown. The dashed lines represent simulations where volcanic influence is taken into account. (b) Same as (a) for the year 1980. The respective horizontal distribution is shown in Figure 6 for 1979.

ilar values in the aerosol concentrations at these altitudes and in this area. This suggests that the ATAL 1979 was not significantly influenced by volcanic eruptions. A model simulation for 1980 was conducted and shows an ATAL signal with a similar magnitude as observed in Figure 5a. Simulations taking volcanic emissions (i.e. from Mount Saint Helens eruption) into consideration show very different sulfate and NH_4 aerosols vertical shapes, with substantially increased concentrations. This is a result of the formation of secondary sulfate and ammonium-sulfate aerosols initiated by volcanic SO_2 emissions.

In Figure 6 we show the horizontal distribution of our ATAL simulations for 1979. This reveals a typical horizontal ATAL structure for the different types of aerosols in the model, with maxima mass concentration values within the AMA boundaries. Simulations suggest that mass concentration values for sulfates, POM (Primary Organic Aerosol), BC (Black Carbon) and ammonium have approximately doubled in the 2010s with respect to 1979 and 1980 (compared to the modeled ATAL of 2000-2015 from Bossolasco et al. (2021). The increasing ATAL signature with time can be explained by enhancing pollution and anthropogenic emissions in and around Asia during the past decades. Surface emissions of human-made SO_2, SO_4 (from agriculture, solvents, waste and residential, transportation), POM and NH_3 steadily increase between 1980 and 2015, according to MERRA-2 data. For SO_2 and NH_3, we find increases of 40-100%. The corresponding trends in anthropogenic emissions between 1980 and 2015 for India are shown in Figure 7. Main source regions responsible for the ATAL and its composition have been found to be located in India, including North India and South of the Tibetan Plateau (e.g. Tissier & Legras, 2016; Legras & Bucci, 2020; Clemens et al., 2023). Simulated mineral dust components, which are not directly influenced by human activities, do not show an increasing trend from 1979 to the 2010 decade. Dust is largely the dominant aerosol type, by mass concentration, in our ATAL simulations (up to a factor 10 larger than sulfate aerosols).

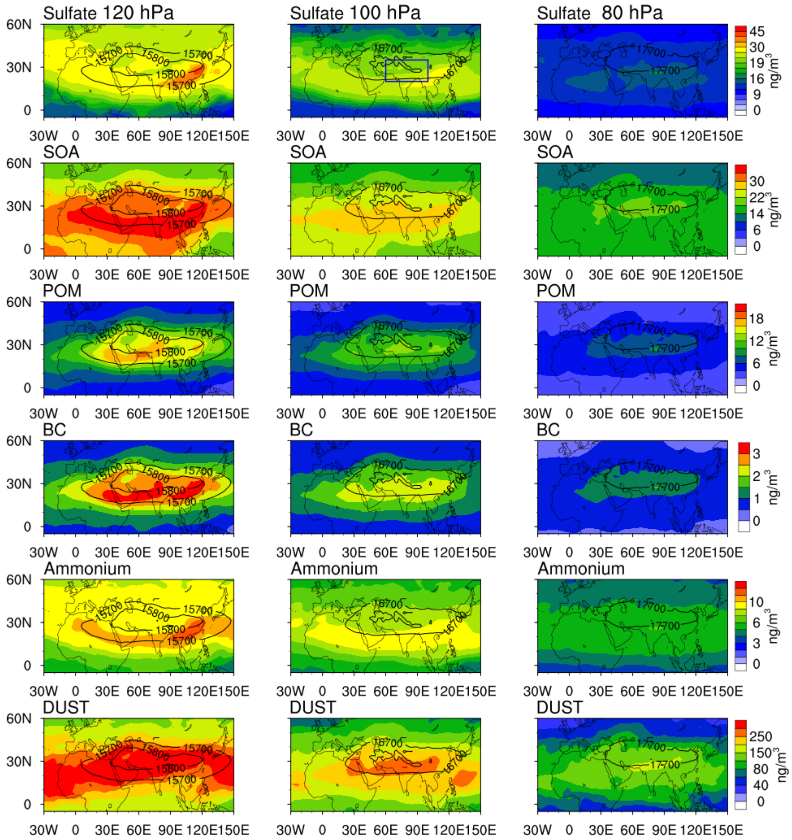

Figure 6. Graphical distribution of aerosol mass concentration, from model simulations, averaged for July/August 1979 for the 5 aerosol components presented in Figure 5a and mineral dust, at 120 (left column), 100 (center column) and 80 hPa (right column) pressure levels. Geopotential levels are indicated by black lines. The blue box in the second panel represents the averaging area used for Figure 5b.

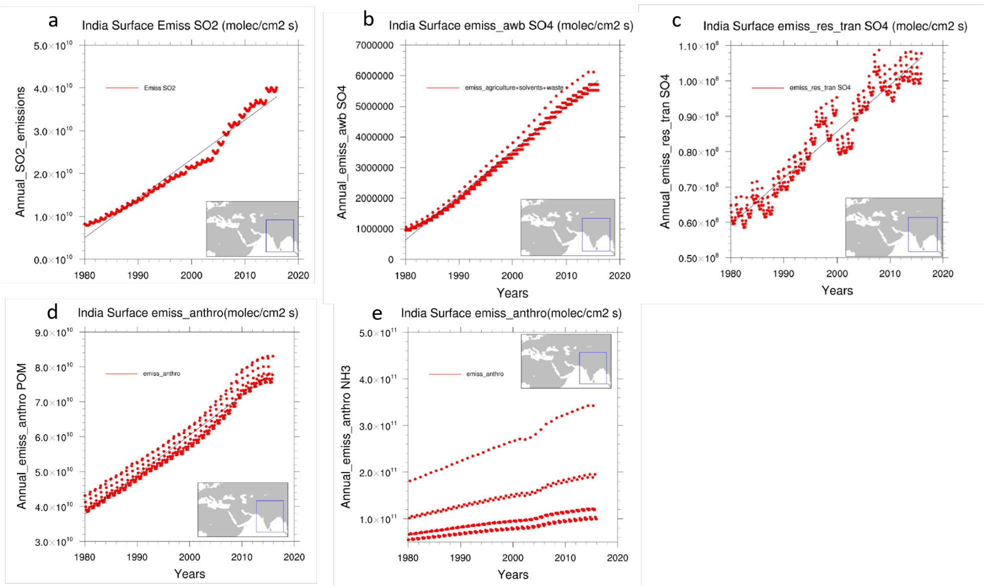

Figure 7. MERRA-2 trend analysis for human made emissions from India (box 0-40°N, 65-95°E) 1980-2015 for (a) SO_2, (b) SO_4 agriculture+solvents+waste, (c) SO_4 residential+transportation, (d) Primary Organic Aerosol POM and (e) NH_3.

4 Discussion

While model simulations (and in situ observations in 2017) point to the existence of a weak, but significant ATAL signal, the SAGE I, II and III/ISS data records show no statistically significant ATAL structure compared to observations outside the AMA, when averaging over the Asian monsoon time frame.
The ability to confidently identify ATAL related aerosol using limb data such as SAGE is limited by a number of factors:

- There are relatively few observation opportunities in the ATAL spatial region that, particularly for solar occultation, only occur episodically through the ATAL seasonal life span.
- The high number of clouds that occur in the ATAL region, particularly during the ATAL season due to systematic convective outflow, can result in the loss of observations in the core of this region where the largest and most easily identified aerosol enhancements may occur. As a result, the inference of the presence of enhanced aerosol is dependent on how robustly aerosol can be distinguished from the cloud/aerosol mixtures that are characteristic of SAGE observations globally. Ultimately, this would be straightforward if the ATAL aerosol is primarily the result of the nucleation of new small aerosol from aerosol precursors in a way that mimics small to moderate volcanic activity that increase (or maintain) the 525 to 1020 nm aerosol coefficient extinction ratio (Thomason et al., 2021). Conversely, if the aerosol precursors primarily condense on existing aerosol or existing aerosol is transported from the lower troposphere primarily as relatively large aerosol as the ATAL enhancement, then the optical properties of these aerosol can effectively mimic cloud/aerosol mixture in which enhancements in extinction coefficient are tied with decreases in aerosol extinction coefficient ratio. In this case, separating between what is a 'cloud' and what is ATAL would be extremely difficult.
- Furthermore, groups of consecutive SAGE III profile observations within the AMA box appear usually within a time frame of a few days and within a few degrees

of longitude. In other words, most of the averaged profiles within one ATAL season mostly originate from a short time frame (within days) at similar latitudes. The ATAL is a patchy feature and depends strongly on the AMA dynamics each season, which is also demonstrated by the contrasting compositions of the ATAL during different measurements campaigns. Hence, we do not expect that the sampling of a solar occultation instrument is sufficient to give a representative average of the ATAL during the whole AMA season.

- Generally, an increase of the ATAL signal with time is expected, because of increasing anthropogenic emissions in Asia (Fadnavis et al., 2013; Neely et al., 2014; Bossolasco et al., 2021). Therefore, a weaker extinction enhancement in the early 1990s and before is expected and confirmed with the CAM5-MAM7 simulations (Figure 5 and 6). A lower ATAL signal in (potentially) individual profiles makes it even more unlikely to show an ATAL structure for earlier years within the SAGE record.
- Space LiDAR observations or limb observations with significantly higher sampling such as CALIOP and OMPS, are expected to be better suitable for potential ATAL evolution studies. However, their respective time series is not long enough for ATAL investigations in and before the 1990s.

5 Conclusions

Space-borne solar occultation observations within the Asian monsoon region are not suitable for the representation of quantitative averaged values, for a highly variable ATAL in space and time during each season. Averages over a given geographical box (both in and out of the ATAL) may drown the ATAL signal while apparent on some individual profiles. SAGE (I, II and III/ISS) aerosol extinction observations (past and present) can therefore neither be used for any kind of trend analysis, nor to exclude the existence of the ATAL for specific years, as it was done in previous studies (e.g. V15, Thomason and Vernier (2013)). The same is expected for quantitative, trend analysis of trace gases within the AMA, using solar occultation observations (e.g. from the Atmospheric Chemistry Experiment Fourier Transform Spectrometer, ACE-FTS).
Averaged SAGE I and II observations for the years 1979 to 2005 can neither confirm nor deny the presence of an ATAL signal and it is impossible to point the first existence of the ATAL to a specific time frame and specific location/region, based on available space-borne observations. On the contrary, individual profiles, with applied cloud filter, within the transport barrier of the AMA, can potentially point to an ATAL signal. However, we find that such features are also observed far outside the ATAL boundaries and season and therefore not highly reliable.
While space-borne observations cannot be used for early investigations of the existence and trend of the annually appearing ATAL, we are left to rely on model simulations. CAM5-MAM7 simulations show a clear ATAL signal for both tested years (1979 and 1980), consisting of both natural appearing aerosols (e.g. dust) and from human-made emissions (e.g. sulfates, organics, ammonium). A detailed simulation-based ATAL evolution analysis starting from pre industrial years to the early 2000s is planned as a follow-up study.

Open Research Section

SAGE I, SAGE II and SAGE III/ISS can be obtained at https://eosweb.larc.nasa.gov
.

Acknowledgments

CK was funded by the German Research Foundation, DFG (409585735). CK, PS, BL,GB, FJ and AB acknowledge the support of the Agence Nationale de La Recherche ANR TTL-XING (ANR-17-CE01-0015). We acknowledge the discussion and help from the SAGE science team at NASA-Langley and would like to thank all the teams and scientists involved in the whole process of data production for SAGE (I – III/ISS). Furthermore, we thank Jean-Paul Vernier for his help and discussions. We would like to thank Marc von Hobe for discussion and technical support.

References

Appel, O., Köllner, F., Dragoneas, A., Hünig, A., Molleker, S., Schlager, H., ... Borrmann, S. (2022). Chemical analysis of the asian tropopause aerosol layer (atal) with emphasis on secondary aerosol particles using aircraft based in situ aerosol mass spectrometry. *Atmospheric Chemistry and Physics Discussions*, *2022*, 1–37. Retrieved from `https://acp.copernicus.org/preprints/acp-2022-92/` doi: 10.5194/acp-2022-92

Bossolasco, A., Jegou, F., Sellitto, P., Berthet, G., Kloss, C., & Legras, B. (2021). Global modeling studies of composition and decadal trends of the asian tropopause aerosol layer. *Atmospheric Chemistry and Physics*, *21*(4), 2745–2764. Retrieved from `https://acp.copernicus.org/articles/21/2745/2021/` doi: 10.5194/acp-21-2745-2021

Brunamonti, S., Jorge, T., Oelsner, P., Hanumanthu, S., Singh, B. B., Kumar, K. R., ... Peter, T. (2018). Balloon-borne measurements of temperature, water vapor, ozone and aerosol backscatter on the southern slopes of the himalayas during stratoclim 2016–2017. *Atmospheric Chemistry and Physics*, *18*(21), 15937–15957. Retrieved from `https://acp.copernicus.org/articles/18/15937/2018/` doi: 10.5194/acp-18-15937-2018

Chu, W., & McCornick, M. (1979). Inversion of stratospheric aerosol and gaseous constituents from spacecraft solar extinction data in the 0.38-1.0-microm wavelength region. *Appl Opt.*, *18*(9), 1404-13. doi: 10.1364/AO.18.001404

Clemens, J., Vogel, B., Hoffmann, L., Griessbach, S., Thomas, N., Fadnavis, S., ... Ploeger, F. (2023). Identification of source regions of the asian tropopause aerosol layer on the indian subcontinent in august 2016. *EGUsphere*, *2023*, 1–39. Retrieved from `https://egusphere.copernicus.org/preprints/2023/egusphere-2022-1462/` doi: 10.5194/egusphere-2022-1462

Damadeo, R. P., Zawodny, J. M., & Thomason, L. W. (2014). Reevaluation of stratospheric ozone trends from sage ii data using a simultaneous temporal and spatial analysis. *Atmospheric Chemistry and Physics*, *14*(24), 13455–13470. Retrieved from `https://acp.copernicus.org/articles/14/13455/2014/` doi: 10.5194/acp-14-13455-2014

Damadeo, R. P., Zawodny, J. M., Thomason, L. W., & Iyer, N. (2013). Sage version 7.0 algorithm: application to sage ii. *Atmospheric Measurement Techniques*, *6*(12), 3539–3561. Retrieved from `https://amt.copernicus.org/articles/6/3539/2013/` doi: 10.5194/amt-6-3539-2013

Fadnavis, S., Roy, C., Sabin, T., Ayantika, D. C., & Ashok, K. (2017). Potential modulations of pre-monsoon aerosols during el niño: impact on indian summer monsoon. *Climate Dynamics*, *49*(7), 1432-0894. Retrieved from `https://doi.org/10.1007/s00382-016-3451-6` doi: 10.1007/s00382-016-3451-6

Fadnavis, S., Sabin, T., Roy, C., Rowlinson, M., Rap, A., Vernier, J.-P., & Sioris, C. (2019). Elevated aerosol layer over south asia worsens the indian droughts. *Scientific Reports*, *9*(1), 2045-2322. Retrieved from `https://doi.org/10.1038/s41598-019-46704-9` doi: 10.1038/s41598-019-46704-9

Fadnavis, S., Semeniuk, K., Pozzoli, L., Schultz, M. G., Ghude, S. D., Das, S., & Kakatkar, R. (2013). Transport of aerosols into the utls and their impact on the asian monsoon region as seen in a global model simulation. *Atmospheric Chemistry and Physics*, *13*(17), 8771–8786. Retrieved from `https://acp.copernicus.org/articles/13/8771/2013/` doi: 10.5194/acp-13-8771-2013

Fairlie, T. D., Liu, H., Vernier, J.-P., Campuzano-Jost, P., Jimenez, J. L., Jo, D. S., ... Huey, G. (2020). Estimates of regional source contributions to the asian tropopause aerosol layer using a chemical transport model. *Journal of Geophysical Research: Atmospheres*, *125*(4), e2019JD031506. Retrieved from https://agupubs.onlinelibrary.wiley.com/doi/abs/10.1029/2019JD031506 (e2019JD031506 2019JD031506) doi: https://doi.org/10.1029/2019JD031506

Hanumanthu, S., Vogel, B., Müller, R., Brunamonti, S., Fadnavis, S., Li, D., ... Peter, T. (2020). Strong day-to-day variability of the asian tropopause aerosol layer (atal) in august 2016 at the himalayan foothills. *Atmospheric Chemistry and Physics*, *20*(22), 14273–14302. Retrieved from https://acp.copernicus.org/articles/20/14273/2020/ doi: 10.5194/acp-20-14273-2020

Höpfner, M., Ungermann, J., Borrmann, S., Wagner, R., Spang, R., Riese, M., ... Wohltmann, I. (2019). Ammonium nitrate particles formed in upper troposphere from ground ammonia sources during asian monsoons. *Nature Geoscience*, *12*(17), 1752-0908. Retrieved from https://doi.org/10.1038/s41561-019-0385-8 doi: 10.1038/s41561-019-0385-8

Kent, G. S., & McCormick, M. P. (1984). Sage and sam ii measurements of global stratospheric aerosol optical depth and mass loading. *Journal of Geophysical Research: Atmospheres*, *89*(D4), 5303-5314. Retrieved from https://agupubs.onlinelibrary.wiley.com/doi/abs/10.1029/JD089iD04p05303 doi: https://doi.org/10.1029/JD089iD04p05303

Kloss, C., Berthet, G., Sellitto, P., Ploeger, F., Bucci, S., Khaykin, S., ... Legras, B. (2019). Transport of the 2017 canadian wildfire plume to the tropics via the asian monsoon circulation. *Atmospheric Chemistry and Physics*, *19*(21), 13547–13567. Retrieved from https://acp.copernicus.org/articles/19/13547/2019/ doi: 10.5194/acp-19-13547-2019

Kovilakam, M., Thomason, L. W., Ernest, N., Rieger, L., Bourassa, A., & Millán, L. (2020). The global space-based stratospheric aerosol climatology (version 2.0): 1979–2018. *Earth System Science Data*, *12*(4), 2607–2634. Retrieved from https://essd.copernicus.org/articles/12/2607/2020/ doi: 10.5194/essd-12-2607-2020

Lau, W., Yuan, C., & Li, Z. (2018). Origin, maintenance and variability of the asian tropopause aerosol layer (atal): The roles of monsoon dynamics. *Scientific Reports*, *8*(1), 2045-2322. Retrieved from https://doi.org/10.1038/s41598-018-22267-z doi: 10.1038/s41598-018-22267-z

Legras, B., & Bucci, S. (2020). Confinement of air in the asian monsoon anticyclone and pathways of convective air to the stratosphere during the summer season. *Atmospheric Chemistry and Physics*, *20*(18), 11045–11064. Retrieved from https://acp.copernicus.org/articles/20/11045/2020/ doi: 10.5194/acp-20-11045-2020

Liu, X., Easter, R. C., Ghan, S. J., Zaveri, R., Rasch, P., Shi, X., ... Mitchell, D. (2012). Toward a minimal representation of aerosols in climate models: description and evaluation in the community atmosphere model cam5. *Geoscientific Model Development*, *5*(3), 709–739. Retrieved from https://gmd.copernicus.org/articles/5/709/2012/ doi: 10.5194/gmd-5-709-2012

Liu, X., Zhang, X., Huang, Y., Chen, K., Wang, L., Ma, J., ... Luo, J. (2021). The direct radiative forcing impact of agriculture-emitted black carbon associated with india's green revolution. *Earth's Future*, *9*(6), e2021EF001975. Retrieved from https://agupubs.onlinelibrary.wiley.com/doi/abs/10.1029/2021EF001975 (e2021EF001975 2021EF001975) doi: https://doi.org/10.1029/2021EF001975

Ma, J., Brühl, C., He, Q., Steil, B., Karydis, V. A., Klingmüller, K., ... Lelieveld, J. (2019). Modeling the aerosol chemical composition of the tropopause over the tibetan plateau during the asian summer monsoon. *Atmospheric Chemistry and Physics*, *19*(17), 11587–11612. Retrieved from https://acp.copernicus.org/articles/19/11587/2019/ doi: 10.5194/acp-19-11587-2019

Mahnke, C., Weigel, R., Cairo, F., Vernier, J.-P., Afchine, A., Krämer, M., ... Borrmann, S. (2021). The atal within the 2017 asian monsoon anticyclone: Microphysical aerosol properties derived from aircraft-borne in situ measurements. *Atmospheric Chemistry and Physics Discussions*, *2021*, 1–31. Retrieved from https://acp.copernicus.org/preprints/acp-2020-1241/ doi: 10.5194/acp-2020-1241

McCormick, M. P., Hamill, P., Pepin, T. J., Chu, W. P., Swissler, T. J., & McMaster, L. R. (1979). Satellite studies of the stratospheric aerosol. *BAMS*, *60*(9), 1038-1046. Retrieved from http://www.jstor.org/stable/26219219

Neely, R. R., Yu, P., Rosenlof, K. H., Toon, O. B., Daniel, J. S., Solomon, S., & Miller, H. L. (2014). The contribution of anthropogenic so2 emissions to the asian tropopause aerosol layer. *Journal of Geophysical Research: Atmospheres*, *119*(3), 1571-1579. Retrieved from https://agupubs.onlinelibrary.wiley.com/doi/abs/10.1002/2013JD020578 doi: https://doi.org/10.1002/2013JD020578

Pan, L. L., Honomichl, S. B., Kinnison, D. E., Abalos, M., Randel, W. J., Bergman, J. W., & Bian, J. (2016). Transport of chemical tracers from the boundary layer to stratosphere associated with the dynamics of the asian summer monsoon. *Journal of Geophysical Research: Atmospheres*, *121*(23), 14,159-14,174. Retrieved from https://agupubs.onlinelibrary.wiley.com/doi/abs/10.1002/2016JD025616 doi: https://doi.org/10.1002/2016JD025616

Pingali, P. L. (2012). Green revolution: Impacts, limits, and the path ahead. *Proceedings of the National Academy of Sciences*, *109*(31), 12302–12308. Retrieved from https://www.pnas.org/content/109/31/12302 doi: 10.1073/pnas.0912953109

Ploeger, F., Gottschling, C., Griessbach, S., Grooß, J.-U., Guenther, G., Konopka, P., ... von Hobe, M. (2015). A potential vorticity-based determination of the transport barrier in the asian summer monsoon anticyclone. *Atmos Chem Phys*, *15*(22), 13145–13159. Retrieved from https://www.atmos-chem-phys.net/15/13145/2015/ doi: 10.5194/acp-15-13145-2015

Russell, J. (1981). *Middle atmosphere program: Handbook for map.* International Council of Scientific Unions. Scientific Committee on Solar-Terrestrial Physics and United States. National Aeronautics and Space Administration. Retrieved from https://books.google.de/books?id=U3S2byB_44YC

Russell, P. B., McCormick, M. P., Swissler, T. J., Rosen, J. M., Hofmann, D. J., & McMaster, L. R. (1984). Satellite and correlative measurements of the stratospheric aerosol. iii: Comparison of measurements by sam ii, sage, dustsondes, filters, impactors and lidar. *Journal of Atmospheric Sciences*, *41*(11), 1791 - 1800. Retrieved from https://journals.ametsoc.org/view/journals/atsc/41/11/1520-0469_1984_041_1791_sacmot_2_0_co_2.xml doi: https://doi.org/10.1175/1520-0469(1984)041⟨1791:SACMOT⟩2.0.CO;2

Santee, M. L., Manney, G. L., Livesey, N. J., Schwartz, M. J., Neu, J. L., & Read, W. G. (2017). A comprehensive overview of the climatological composition of the asian summer monsoon anticyclone based on 10 years of aura microwave limb sounder measurements. *Journal of Geophysical Research: Atmospheres*, *122*(10), 5491-5514. Retrieved from https://agupubs.onlinelibrary.wiley.com/doi/abs/10.1002/2016JD026408 doi: https://doi.org/10.1002/2016JD026408

Smith, S. J., van Aardenne, J., Klimont, Z., Andres, R. J., Volke, A., & Delgado Arias, S. (2011). Anthropogenic sulfur dioxide emissions: 1850–2005. *Atmospheric Chemistry and Physics*, *11*(3), 1101–1116. Retrieved from https://acp.copernicus.org/articles/11/1101/2011/ doi: 10.5194/

acp-11-1101-2011

Thomason, L. W. (2012). Toward a combined sage ii-haloe aerosol climatology: an evaluation of haloe version 19 stratospheric aerosol extinction coefficient observations. *Atmospheric Chemistry and Physics*, *12*(17), 8177–8188. Retrieved from `https://acp.copernicus.org/articles/12/8177/2012/` doi: 10.5194/acp-12-8177-2012

Thomason, L. W., Kent, G. S., Trepte, C. R., & Poole, L. R. (1997). A comparison of the stratospheric aerosol background periods of 1979 and 1989–1991. *Journal of Geophysical Research: Atmospheres*, *102*(D3), 3611-3616. Retrieved from `https://agupubs.onlinelibrary.wiley.com/doi/abs/10.1029/96JD02960` doi: https://doi.org/10.1029/96JD02960

Thomason, L. W., Kovilakam, M., Schmidt, A., von Savigny, C., Knepp, T., & Rieger, L. (2021). Evidence for the predictability of changes in the stratospheric aerosol size following volcanic eruptions of diverse magnitudes using space-based instruments. *Atmospheric Chemistry and Physics*, *21*(2), 1143–1158. Retrieved from `https://acp.copernicus.org/articles/21/1143/2021/` doi: 10.5194/acp-21-1143-2021

Thomason, L. W., & Vernier, J.-P. (2013). Improved sage ii cloud/aerosol categorization and observations of the asian tropopause aerosol layer: 1989-2005. *Atmospheric Chemistry and Physics*, *13*(9), 4605–4616. Retrieved from `https://acp.copernicus.org/articles/13/4605/2013/` doi: 10.5194/acp-13-4605-2013

Tissier, A.-S., & Legras, B. (2016). Convective sources of trajectories traversing the tropical tropopause layer. *Atmospheric Chemistry and Physics*, *16*(5), 3383–3398. Retrieved from `https://acp.copernicus.org/articles/16/3383/2016/` doi: 10.5194/acp-16-3383-2016

Vernier, H., Rastogi, N., Liu, H., Pandit, A. K., Bedka, K., Pa-tel, A., … Vernier, J.-P. (2022). Exploring the inorganic composition of the asian tropopause aerosol layer using medium-duration balloon flights. *Atmospheric Chemistry and Physics*, *22*(18), 12675–12694. Retrieved from `https://acp.copernicus.org/articles/22/12675/2022/` doi: 10.5194/acp-22-12675-2022

Vernier, J.-P., Fairlie, T., Natarajan, M., Deshler, T., Gadhavi, H., Ratnam, M., … Kumar, S. (2018). Batal: The balloon measurement campaigns of the asian tropopause aerosol layer. *BAMS*, *99*(5), 955-973. Retrieved from `https://doi.org/10.1175/BAMS-D-17-0014.1`

Vernier, J.-P., Fairlie, T. D., Natarajan, M., Wienhold, F. G., Bian, J., Martinsson, B. G., … Bedka, K. M. (2015). Increase in upper tropospheric and lower stratospheric aerosol levels and its potential connection with asian pollution. *Journal of Geophysical Research: Atmospheres*, *120*(4), 1608-1619. Retrieved from `https://agupubs.onlinelibrary.wiley.com/doi/abs/10.1002/2014JD022372` doi: https://doi.org/10.1002/2014JD022372

Vernier, J.-P., Thomason, L. W., & Kar, J. (2011). Calipso detection of an asian tropopause aerosol layer. *Geophysical Research Letters*, *38*(7). Retrieved from `https://agupubs.onlinelibrary.wiley.com/doi/abs/10.1029/2010GL046614` doi: https://doi.org/10.1029/2010GL046614

Vernier, J.-P., Thomason, L. W., Pommereau, J.-P., Bourassa, A., Pelon, J., Garnier, A., … Vargas, F. (2011). Major influence of tropical volcanic eruptions on the stratospheric aerosol layer during the last decade. *Geophysical Research Letters*, *38*(12). Retrieved from `https://agupubs.onlinelibrary.wiley.com/doi/abs/10.1029/2011GL047563` doi: https://doi.org/10.1029/2011GL047563

Vogel, B., Günther, G., Müller, R., Grooß, J.-U., & Riese, M. (2015). Impact of different asian source regions on the composition of the asian monsoon anticyclone and of the extratropical lowermost stratosphere. *Atmospheric Chemistry and Physics*, *15*(23), 13699–13716. Retrieved from https://acp.copernicus.org/articles/15/13699/2015/ doi: 10.5194/acp-15-13699-2015

Yu, P., Toon, O. B., Neely, R. R., Martinsson, B. G., & Brenninkmeijer, C. A. M. (2015). Composition and physical properties of the asian tropopause aerosol layer and the north american tropospheric aerosol layer. *Geophysical Research Letters*, *42*(7), 2540-2546. Retrieved from https://agupubs.onlinelibrary.wiley.com/doi/abs/10.1002/2015GL063181 doi: https://doi.org/10.1002/2015GL063181

Yuan, C., Lau, W. K. M., Li, Z., & Cribb, M. (2019). Relationship between asian monsoon strength and transport of surface aerosols to the asian tropopause aerosol layer (atal): interannual variability and decadal changes. *Atmospheric Chemistry and Physics*, *19*(3), 1901–1913. Retrieved from https://acp.copernicus.org/articles/19/1901/2019/ doi: 10.5194/acp-19-1901-2019